Contribution of the incudo-malleolar joint to middle-ear sound transmission

Gerig, Rahel ; Ihrle, Sebastian ; Röösli, Christof ; Dalbert, Adrian ; Dobrev, Ivo ; Pfiffner, Flurin ; Eiber, Albrecht ; Huber, Alexander M ; Sim, Jae Hoon

DOI: https://doi.org/10.1016/j.heares.2015.07.011

CONTRIBUTION OF THE INCUDO-MALLEOLAR JOINT TO MIDDLE-EAR SOUND TRANSMISSION

[1]Rahel Gerig*, [2]Sebastian Ihrle, [1]Christof Röösli, [1]Adrian Dalbert, [1]Ivo Dobrev, [1]Flurin Pfiffner, [2]Albrecht Eiber, [1]Alexander M. Huber, [1]Jae Hoon Sim

[1]*University Hospital Zurich, University of Zurich,* [2]*University of Stuttgart*

*Corresponding author e-mail address: MEM_ENT@usz.ch

Abstract

The malleus and incus in the human middle ear are linked by the incudo-malleolar joint (IMJ). The mobility of the human IMJ under physiologically relevant acoustic stimulation and its functional role in middle-ear sound transmission are still debated. In this study, spatial stapes motions were measured during acoustic stimulation (0.25-8 kHz) in six fresh human temporal bones for two conditions of the IMJ: (1) normal IMJ and (2) IMJ with experimentally-reduced mobility. Stapes velocity was measured at multiple points on the footplate using a scanning laser Doppler vibrometry (SLDV) system, and the 3D motion components were calculated under both conditions of the IMJ. The artificial reduction of the IMJ mobility was confirmed by measuring the relative motion between the malleus and the incus. The magnitudes of the piston-like motion of the stapes increased with the reduced IMJ mobility above 2 kHz. The increase was frequency dependent and was prominent from 2-4 kHz and at 5.5 kHz. The magnitude ratios of the rocking-like motions to the piston-like motion were similar for both IMJ conditions. The frequency-dependent change of the piston-like motion after the reduction of the IMJ mobility suggests that the IMJ is mobile under physiologically relevant levels of acoustic stimulation, especially at frequencies above 2 kHz.

Keywords: Incudo-malleolar joint (IMJ); incudo-malleal joint (IMJ); malleo-incudal joint; incudo-mallear joint; articulatio incudomallearis; middle ear; malleus; incus; stapes; piston-like motion; rocking-like motion; Laser Doppler Vibrometer (LDV); micro-CT

Abbreviations: **3D**: three dimensional; **AEC**: artificial ear canal; **IMJ**: incudo-malleolar joint; **ISJ**: incudo-stapedial joint; **LDV**: laser Doppler vibrometry; **Micro-CT**: micro–computed tomography; **SLDV**: scanning laser Doppler vibrometry; **TB**: temporal bone; **TM:** tympanic membrane

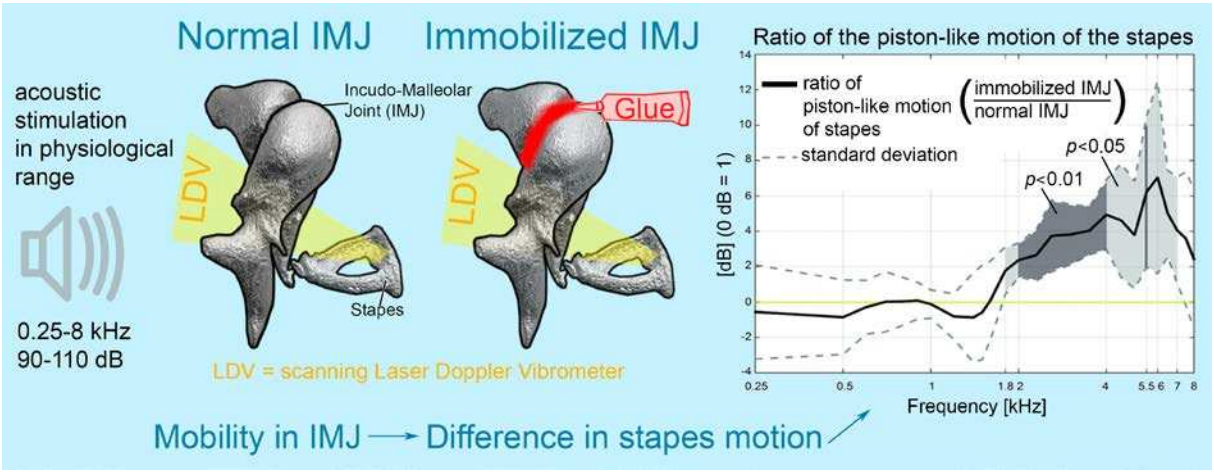

1. Introduction

The ossicular chain in the human middle ear transmits sound-induced mechanical vibrations of the tympanic membrane (TM) to the inner ear. The middle-ear ossicular chain comprises three bones -- the malleus, incus, and stapes, which are connected via the incudo-malleolar joint (IMJ) and incudo-stapedial joint (ISJ).

The IMJ connects the articular surfaces of the malleus and incus and has a twisted saddle shape (Helmholtz 1863; Etholm and Belal, 1974; Sim and Puria, 2008). It has previously been described in the literature as a synovial joint (diarthrodial joint/diarthrosis) (Politzer, 1884; Harty, 1953, 1964; Etholm and Belal, 1974; Schuknecht, 1974; Marquet, 1981; Hüttenbrink and Pfautsch, 1987; FICAT, 1998; Sim and Puria, 2008). According to the literature, the IMJ is encapsulated by fibrous structures along its borders and contains synovial fluid inside the capsule, without the muscular components that are present in skeletal joints. The thickness of the IMJ tissue structures between the articular surfaces of the malleus and the incus varies from 0.04 mm to 0.32 mm along the intra-articular space, with maximal thickness on the medial and lateral aspects (Sim and Puria, 2008). The anatomical features of the IMJ may allow it to be deformed, resulting in relative motions between the malleus and incus.

The role of the IMJ as a protection mechanism against large static pressure changes has been proposed. For example, Kirikae (1960) argued that the IMJ is immobile up to 140 dB SPL, after which relative motion between the malleus and the incus could occur. Hüttenbrink (1988a) found that the IMJ is mobile under static pressure change. Such relative shear motions between the malleus and incus in human temporal bones (TBs) has been found in other studies as well (Kobrak, 1959; Cancura, 1980; Hüttenbrink, 1988b; Dahmann, 1929; Politzer, 1873; Mach and Kessel, 1874).

While relative displacement between the malleus and the incus under static pressure change of large magnitudes is generally accepted, flexibility of the human IMJ under acoustic

62 stimulation at physiologically-relevant levels and its functional role in middle-ear sound
63 transmission are still under debate.

64 Several previous works have proposed frequency-dependent behavior of the IMJ,
65 which allows considerable relative motion between the malleus and incus only for the high
66 frequencies. Elpern et al. (1965) observed relative motion above 4 kHz in human TBs, Guinan
67 and Peake (1967) more relative motions at "higher frequencies" in cats and Willi et al. (2002)
68 above 2 kHz in human TBs. Such high-frequency dominant slippage was also observed in
69 three-dimensional measurements of ossicular motion in one human TB (Decraemer and
70 Khanna, 2004). "Slippage" of the IMJ was observed in a study with two human TBs even for
71 the low frequencies (Decraemer and Khanna, 2001), but in their study, the slippage was
72 dominant at the high frequencies.

73 While some previous studies have argued that the IMJ is functionally immobilized
74 during middle-ear sound transmission under physiological acoustic stimulation, the methods
75 used in these studies did not account for factors that we realize today can influence the results
76 resulting in potential inaccuracies. Harty (1964) made predictions based solely on
77 morphological examination. Békésy (1960) used TBs with a drained cochlea in his
78 measurements. It is known that absence of impedance of the cochlear fluid with a drained
79 cochlea results in an increase of the middle-ear transfer function, especially above 0.5 kHz
80 (Gyo et al. 1987). Some measurement systems were in contact with the middle-ear ossicles,
81 which may change the natural motions of the ossicles. One example is a capacitive probe
82 (Békésy, 1941), where a piece of metal foil is attached to measure the vibration of the surface
83 of interest. Gundersen and Hogmoen, (1976) performed their measurements only at
84 frequencies below 2 kHz with time-averaged holographic methods. The measurement with an
85 electromagnetic probe in a study reported by Cancura (1980) was only static and not dynamic.
86 In Elpern et al. (1965), the immobilization of the IMJ was not verified; thus the information of
87 the degree of immobilization was missing.

Willi (2003) and Offergeld et al. (2007) have reported that relative motion between the malleus and the incus caused by the mobility of the IMJ resulted in frequency-dependent transmission loss in the middle-ear transfer function. Willi (2003) observed that immobilizing the IMJ resulted in less transmission loss between the malleus and incus. In this study, after the immobilization of the IMJ, almost no change in transmission was observed below 1.5 kHz, and the transmission increased with frequency above 3 kHz, reaching a 10-dB increase at 10 kHz. Similarly, an increase (less than 10 dB) of stapes motion amplitude occurred in the high frequencies (from 1.2 kHz to 5 kHz) after immobilization of the IMJ, as reported by Offergeld et al. (2007). However, the work by Willi explored transmission loss between the malleus and incus rather than transmission loss through the entire middle ear, which is defined as motion of the stapes with respect to ear-canal pressure. Further, the measurements and analysis were two-dimensional. In the work by Offergeld et al., motions of the stapes were measured one-dimensionally, and immobilization of the IMJ was not quantitatively examined.

In our study, it is hypothesized based on previous studies that the IMJ is mobile under physiological relevant acoustic stimulation, and the mobility of the IMJ results in transmission loss in the middle-ear transfer function, especially at higher frequencies. Our aim is to assess the contribution of the IMJ to middle-ear sound transmission accurately by using current methodologies that include quantification of artificial immobilization of the IMJ and three-dimensional measurement of stapes motion.

2. Material and Methods

Fresh TBs from human cadavers were used in this study, and approval was obtained by the Ethical Committee of Zurich (KEK-ZH-Nr. 2012-0007).

To assess the contribution of the IMJ to middle-ear sound transmission in human ears, spatial motions of the stapes, which were measured using a laser Doppler vibrometry (LDV) system, were compared under two different conditions of the IMJ: (1) normal IMJ and (2) IMJ with experimentally reduced mobility. To reduce the mobility of the IMJ, the articular capsule of the IMJ was opened with a surgical hook on the superior side, and removal of the synovial liquid was facilitated by capillary flow to an absorbent tissue. Then, the cavity was filled with glue (Denseal Superior, Prevest Denpro GmbH, Germany) such that the glue replaced the synovial fluid and connected the articular surfaces of the malleus and the incus. For purposes of the study, we refer to the unmodified IMJ as “mobile IMJ,” and the IMJ with reduced mobility following insertion of the glue (reduced by 15-18 dB, see Fig. 3) as “immobilized IMJ."

The effectiveness of the immobilization of the IMJ was quantified based on the relative motions between the malleus and incus, measured on an area covering the superior parts of the malleus head and the incus body around the IMJ using the LDV system. Once the immobilization was confirmed, spatial motions of the stapes were re-measured and compared to corresponding data with the mobile IMJ. To avoid bias due to physiological changes of middle-ear tissues caused by drying (Rosowski et al., 1990; Voss et al., 2000; Sim et al., 2004), the samples were placed in saline solution for 30 minutes prior to the second stage of the measurement, which was with the immobilized IMJ. The time interval between removing the TBs from the saline solution and the measurements was kept constant at approximately 20 minutes for both stages of the measurement.

2.1 Temporal Bone Preparation

The fresh TBs were harvested within 24 hours after death and were preserved in thiomersal 0.1 % (thimerosal, $C_9H_9HgNaO_2S$) solution at 4° C. Subsequent measurements were done within 7 days after the TBs were harvested (except for TB 2, which was done at 13 days). One TB, which did not conform with the American Society for Testing and Materials (ASTM) standard (F2504-05, Philadelphia, 2005), was excluded during the first stage of the measurements, resulting in a total of six TBs. The six fresh TBs were from four males and two females, with an average age of 68.2 years (ranging from 48 to 83 years).

Exposure of the middle-ear ossicular chain, which included a near-perpendicular view of the stapes footplate and a superior-medial view of the malleus-incus complex, was made by a mastoidectomy with posterior tympanotomy. The TM, middle-ear ossicles, ligaments, and tendon were left intact. The external ear canal was removed and was replaced by an artificial ear canal (AEC) of about 0.5-ml volume (diameter of 9.65 mm and length of 6-8 mm) (Sim et al., 2010, 2012; Lauxmann et al., 2012).

2.2 Acoustical stimulation and measurements of ossicular motion

The stapes motions were measured with harmonic excitations at 26 different frequencies in the range of 0.25 to 8 kHz. The excitation signals were provided by a signal generator incorporated within the PSV data acquisition system (Polytec GmbH, Germany). The stimulation, amplified by an amplifier (RMX 850, QSC Audio Products, USA), was delivered by a loudspeaker (ER-2, Etymotic Research, USA) embedded in the AEC. The sound pressure level (SPL) in the AEC was in the range of 90 – 110 dB SPL, measured by a microphone probe (ER-7C, Etymotic Research, USA).

To obtain the spatial components of the stapes motion, velocities at multiple points (approximately 100 points) on the stapes footplate were measured by a scanning laser Doppler vibrometry (SLDV) system (OFV-3001 SLDV system, Polytec GmbH, Germany). To improve the signal-to-noise ratio of the SLDV, retro-reflective glass beads (50 microns)

were attached to the stapes footplate. A video camera (VCT 24), oriented coaxially with the laser beam, was used to determine the measurement area on the footplate as well as the 2D coordinates (i.e., *X* and *Y* coordinates) of the measurement points in the SLDV measurement frame (corresponds to *XYZ* coordinate system in Fig. 1). In the SLDV measurement frame, the *XYZ* coordinate system was set such that the laser beam was along the *Z* direction and the *XY* plane was normal to the laser beam. The angle θ between the laser beam direction (i.e., *Z* axis of SLDV frame) and the *z* axis of the anatomical frame (see Fig. 1) was 34 ± 11 °.

The mobility of the IMJ was monitored before and after immobilization. Motions of the malleus and incus were measured from a superior-medial view at about 150 points, covering areas on the malleus head and incus body adjacent to the IMJ. The number of measurement points for the malleus and the incus were approximately equal. The acoustic stimulation was by harmonic signals at 0.5, 1, 2, 4, and 6 kHz, in the range of 90 – 110 dB SPL where motions of the human middle-ear ossicular chain as a function of stimulation level are presumed to be linear (Schön and Müller, 1999).

All measurement procedures were controlled by PSV V9.0 software (Polytec GmbH, Germany), and were automated by a custom-made macro within the PSV V9.0 software.

2.3 Registration into anatomical frame (footplate-fixed frame)

After the two stages of the motion measurements of the stapes, all the temporal bones were imaged using the micro-CT 40 (SCANCO Medical AG, Switzerland), with resolutions of 15-18 μm. The 3D features of the stapes were reconstructed from the micro-CT images, and the footplate-fixed anatomical frame (corresponds to *xyz* coordinate system in Fig. 1) of each temporal bone was obtained, such that the *xy*-plane was fitted to the median surface of the corresponding stapes footplate, and the origin was located at the centroid of the median surface. The anterior direction was set as the positive *x*-direction, the superior direction as the positive *y*-direction, and lateral direction as the positive *z*-direction. Thereby, a right-handed

186 frame system was made for the right ear (Fig. 1) and a left-handed frame system for the left
187 ear.
188 To correlate *XYZ* coordinates in the SLDV measurement frame with *xyz* coordinates in
189 the footplate-fixed frame, four or five reference markers (copper wires of 0.75-mm diameter)
190 were glued to the peripheral bones, and the *XY* coordinates of their outlines in the SLDV
191 measurement frame were recorded. The 3D features of the reference markers were also
192 obtained from micro-CT images, and the correlation between the two frames was calculated
193 such that the outline of the reference markers recorded in the SLDV measurement frame was
194 fitted to the outline of the 3D features from the micro-CT images. Once the correlation
195 between the two frames was obtained, the measurement points and measured velocities at
196 those points in the SLDV measurement frame were registered into the footplate-fixed frame,
197 in order to calculate the 3-D motion components of the stapes in the footplate-fixed frame.
198 Details of the frame registration procedures have been described previously (Sim et al., 2010,
199 2012).
200
201 *2.4 Transfer function of the middle ear*
202 Spatial motion components of the stapes were calculated by a method that we have
203 used previously (Sim et al., 2010), in which the translation of the footplate's center along the
204 medial-lateral direction (*z*-direction; piston-like motion, V_{oz}) and two rotations about the long
205 (*x*-direction) and short (*y*-direction) axes of the footplate (rocking-like motions) were
206 considered as the dominant rigid-body motion components of the stapes (Lauxmann et al.,
207 2012). Consequently, the velocities of the three rigid-body motion components were
208 normalized by the measured ear-canal pressure to obtain the corresponding transfer-function
209 components.
210
211 *2.5 Quantification of the IMJ mobility*

212 To quantify the relative motion between the malleus and the incus before and after the
213 IMJ immobilization, the relative motion around the IMJ was measured from a superior view,
214 and the magnitude ratios of the relative motion components to the corresponding motion
215 components of the malleus and incus (R_{vO}, $R_{\omega X}$, $R_{\omega Y}$, and R_{TOTAL}) were obtained.
216 The SLDV system was positioned for the right ear such that the approximate
217 alignments of the direction of each axis were: the *X*-axis, posterior-to-anterior; the *Y*-axis,
218 lateral-to-median; the *Z*-axis, the inferior-to-superior. Since the motions of the malleus and
219 the incus were measured with only one laser beam direction, only three rigid-body motion
220 components for each of the malleus and incus could be obtained in the SLDV measurement
221 frame: translation along the laser beam direction (Z-direction) and two rotations about the *X*-
222 and *Y*-axes of the SLDV measurement frame (Note that the SLDV measurement frame here
223 has nothing to do with either the SLDV measurement frame or the anatomical frame in stapes
224 motion shown in Fig. 1). The translational motion along the laser beam direction was
225 calculated with respect to the center of the measurement area (denoted as *O*), which was
226 located on the IMJ, for both the malleus and the incus. Next, the relative motions in the three
227 rigid body motion components were calculated by

228 $$\left|V_{OR}\right| = \left|V_{OM} - V_{OI}\right|,$$

229 $$\left|\omega_{XR}\right| = \left|\omega_{XM} - \omega_{XI}\right|,$$

230 $$\left|\omega_{YR}\right| = \left|\omega_{YM} - \omega_{YI}\right|, \qquad (1)$$

231 where V_{OM}, $\omega_{XM,}$ and ω_{YM} are the translational velocity of the point *O* along the laser beam
232 direction and two rotational velocities for the malleus, V_{OI}, $\omega_{XI,}$ and ω_{YI} are the translational
233 velocity of the point *O* along the laser beam direction and two rotational velocities for the
234 incus, and V_{OR}, $\omega_{XR,}$ and ω_{YR} are the corresponding relative velocities. In calculation of Eq.
235 (1), all the velocity components were treated as complex numbers to consider the phases.
236 Then, each relative motion component was normalized by the magnitude of the corresponding

motion component of the malleus and incus, as an index representing the ratio of the relative motion to motion of the malleus and incus (R_{vO}, $R_{\omega X}$, and $R_{\omega Y}$).

$$R_{vO} = \frac{|V_{OR}|}{(|V_{OM}| + |V_{OI}|)/2},$$

$$R_{\omega X} = \frac{|\omega_{XR}|}{(|\omega_{XM}| + |\omega_{XI}|)/2},$$

$$R_{\omega Y} = \frac{|\omega_{YR}|}{(|\omega_{YM}| + |\omega_{YI}|)/2}. \quad (2)$$

In Eq. (2), the magnitudes of the corresponding motion components of the malleus and incus were obtained as the average of magnitudes of the malleus motion components and the incus motion components. To represent the ratio of the total relative motion to the incus and malleus motion, the ratios of the relative motion components were averaged with the ratio components weighted by portions of the corresponding motion components.

$$R_{TOTAL} = W_{vO}R_{vO} + W_{\omega X}R_{\omega X} + W_{\omega Y}R_{\omega Y}, \quad (3)$$

In Eq. (3), W_{vO}, $W_{\omega X}$, and $W_{\omega Y}$ indicate weighting coefficients of $|V_{OR}|$, $|\omega_{XR}|$, and $|\omega_{YR}|$, which are calculated by portions of the corresponding motion components.

$$W_{vO} = \frac{|V_{OM}| + |V_{OI}|}{D},$$

$$W_{\omega X} = \frac{|\omega_{XM}| \cdot |\overline{Y}_M| + |\omega_{XI}| \cdot |\overline{Y}_I|}{D},$$

$$W_{\omega Y} = \frac{|\omega_{YM}| \cdot |\overline{X}_M| + |\omega_{YI}| \cdot |\overline{X}_I|}{D},$$

with $D = (|V_{OM}| + |V_{OI}|) + (|\omega_{XM}| \cdot |\overline{Y}_M| + |\omega_{XI}| \cdot |\overline{Y}_I|) + (|\omega_{YM}| \cdot |\overline{X}_M| + |\omega_{YI}| \cdot |\overline{X}_I|)$,

where $|\overline{Y}_M|$ and $|\overline{Y}_I|$ are average distances of measurement points from the center point O in the Y direction, and $|\overline{X}_M|$ and $|\overline{X}_I|$ are average distances of measurement points from the center point O in the X direction, for the malleus and the incus. The multiplication of the

257 average distances to the magnitudes of the corresponding rotational velocity components was
258 done in order to make the magnitudes of the rotational velocity components equivalent to the
259 magnitudes of the translational velocity components.
260
261 *2.6 Statistical analysis*
262 Frequency-dependence and age-dependence of the normal IMJ mobility were analyzed
263 using an ANOVA for repeated measures (with age as covariate for examination of age
264 dependence). Frequency-dependence and age-dependence of the relative change of the
265 piston-like motion between the mobile and immobilized conditions of the IMJ were also
266 analyzed using an ANOVA for repeated measures (with age as covariate for examination of
267 age dependence), with the two variables as the IMJ condition (i.e., mobile and immobilized)
268 and frequency. Data were logarithmically transformed for this analysis. Deviations from
269 sphericity were addressed using the Greenhouse-Geisser correction. Post-hoc comparison
270 with paired *t*-tests was performed for comparison between the mobile and immobilized
271 conditions of the IMJ at each frequency. The statistical calculations were done with SPSS 20
272 software (IBM, USA).

3. Results

3.1 Drying Effect

Figure 2 depicts changes of the motion of the stapes (footplate center) due to drying of the TB tissues. The drying effects were examined in an additional TB, and this TB was not used in the further experiments of the study. The drying effects shown in Fig. 2 are presumed to be similar for all temporal bones. The sample was immersed for 30 minutes in saline solution, and the first measurement (0 min in the figure) took place within 5 minutes after removal from the saline solution. There is a trend for the first natural frequency to increase with time, indicating a stiffening of the suspensory structures due to the drying. The clear phase shift with drying was observed as well. Consequently, over time, there is a reduction in the magnitudes of motions at frequencies below the resonance and an increase of motions above the resonance. The change in the lower frequencies between 90 – 150 minutes of drying was larger than the change during other time intervals. The changes for the higher frequencies were also minimized after 150 minutes. Then, the sample was re-hydrated by immersion in the saline solution for 30 minutes, and the measurement was repeated within 5 minutes after removal from the saline solution ('Rehydration' in the figure). The magnitude of the motion of the stapes with rehydration recovered to approximately the same levels as before drying.

3.2 Immobilization of the IMJ

Figure 3 displays the index for the ratios of the relative motion components between the malleus and the incus to the corresponding motion components of the malleus and incus, calculated using Eqs. (1) - (3), before (solid) and after (dashed) the IMJ was immobilized. Before the IMJ was immobilized, the averaged relative motion ratios (R_{TOTAL}) were small in the low frequency range (-17.5±2.9 dB at 0.5 kHz), and increased with frequency, reaching 0.1±1.9 dB at 6 kHz. The relative motion ratio of ω_Y ($R_{\omega Y}$) was larger than the relative motion

299 ratios of the other components, but its contribution to the weighted average ratio (R_{TOTAL}) was
300 smaller than the contribution of the relative motion ratios of the other components because the
301 motion components ω_{YM} and ω_{YI} of the malleus and incus had smaller magnitudes than other
302 motion components (i.e., $W_{\omega Y}$ was smaller than W_{vO} and $W_{\omega X}$). No dependence of the relative
303 motion on age was observed with the six temporal bones used in this study (ANOVA with age
304 as covariate). After the IMJ was immobilized, the averaged relative motion ratios were
305 reduced by 10 to 15 dB (i.e., R_{TOTAL} was reduced to 18 – 30 % of the values before
306 immobilization of the IMJ), along the frequency range of 0.5 – 6 kHz ($p < 0.05$ at 1 kHz and p
307 < 0.01 at all other frequencies with paired *t*-test). The immobilization of the IMJ was more
308 effective for higher frequencies, where the IMJ had more relative motion before the
309 immobilization (R_{TOTAL} was reduced by 10 dB at 0.5 kHz and by 15 dB at 6 kHz).
310
311 *3.3 Stapes Motion Before/After the IMJ Immobilization*
312 Figure 4 illustrates the magnitude of the translational motions of the footplate's center
313 along the *z*-axis (i.e., piston-like motions, V_{oz}) normalized by the ear canal pressure, before
314 (solid) and after (dashed) the IMJ was immobilized, for all six temporal bones used in this
315 study (TB1-TB6).
316 To determine the effect of the IMJ immobilization on the translational motions,
317 changes of the translational motion with immobilized IMJ relative to the translational motion
318 with mobile IMJ were calculated, and the results are shown in Fig. 5 (relative magnitude
319 ratios (left) and relative phase difference (right)). In the figure, the relative change was
320 calculated for each temporal bone, then the relative changes were averaged over all the
321 temporal bones (n = 6). An ANOVA for repeated measures on the magnitude change revealed
322 that the difference of the magnitude between the two IMJ conditions was frequency-
323 dependent ($p = 0.004$). While the magnitudes were similar for both IMJ conditions at
324 frequencies below 1.8 kHz, the magnitudes were generally higher for the immobilized IMJ for

325 the higher frequencies. The paired *t*-test resulted in *p*-values less than 0.05 for frequencies in
326 the 1.8 to 7 kHz range and *p*-values less than 0.01 for frequencies from 2 to 4 kHz and at 5.5
327 kHz (shaded with dark gray in Fig. 5). The immobilization of the IMJ also tended to cause an
328 increase in phase between 1.5 and 4 kHz. Because of the age range of the TBs and the
329 proposition that mobility could change as a function of age, we examined dependence of the
330 results on age, and no dependence of the relative change on age was observed (ANOVA with
331 age as covariate).

332 To observe the changes in magnitude ratios of the two rotational velocities (i.e.,
333 rocking-like motions) relative to the translational velocities of the footplate-center (i.e.,
334 piston-like motion) following immobilization of the IMJ, the linear velocities at the inferior
335 and posterior edges of the footplate generated by the two rotational velocities were calculated,
336 and were normalized by the footplate-center velocity in the *z*-direction (Heiland et al. 1999;
337 Hato et al. 2003; Sim et al. 2010), for mobile and immobilized IMJ conditions (Fig. 6). The
338 mean values and corresponding standard deviations for each of the mobile and immobilized
339 IMJ conditions were calculated after the relative ratios were obtained for each of the temporal
340 bones (n = 6). The inferior-edge velocities were calculated by multiplication of half of the
341 footplate's short length to the rotational velocity components along the long axis of the
342 footplate, and the posterior-edge velocities by multiplication of half of the footplate's long
343 length to the rotational velocity components along the short axis of the footplate (Sim et al.,
344 2010). The short and long lengths of the footplate were measured from the reconstructed
345 shapes of the stapes, which were obtained from micro-CT imaging for each of the temporal
346 bones. The lengths were 2.86 ± 0.250 mm along the long axis and 1.40 ± 0.101 mm along the
347 short axis, and were slightly longer than the lengths of specimens used in Sim et al. 2013
348 (2.81 ± 0.158 mm along the long axis and 1.27 ± 0.109 mm along the short axis).

349 The mean ratio of the inferior-edge velocity to the footplate-center velocity was
350 approximately -18 dB at 0.25 kHz and increased with frequency, for the both mobile (solid)

and immobilized IMJ (dashed) conditions. The trends were similar for the ratio of the superior-edge velocity to the footplate-center velocity. While Fig. 6 shows the ratios of the edge velocities to the footplate-center velocity separately for each of the mobile and immobilized IMJ conditions, post-hoc comparison with paired *t*-tests was performed for comparison of the ratios between the mobile and immobilized IMJ conditions. No significant difference between the mobile and immobilized IMJ conditions was observed for either the ratio of the inferior-edge velocity to the footplate-center or the ratio of the superior-edge velocity to the footplate-center velocity.

4. Discussion

The goal of this study was to investigate the role of the IMJ in middle-ear sound transmission under physiologically-relevant acoustic stimulation. We controlled for bias due to a drying effect of the TBs in two ways. Each specimen was periodically moistened during the measurements, and the specimens were placed in a saline solution for 30 minutes prior to the measurement with the immobilized IMJ. Previous studies (Rosowski et al. 1990; Voss et al., 2000; Willi et al., 2002; Sim et al., 2004) have reported that physiological changes of the middle-ear tissues due to drying result in significant increase of the resonant frequency of the middle-ear ossicular chain. These studies have also found that the shift of the resonant frequency accelerates with time during a couple of hours at the beginning. Voss et al. (2000) have argued that measurements with TBs are typically presumed to be stable for a "couple of hours," but there is large variability across TBs in the rate of acceleration of the physiological changes of the middle-ear tissues. Our examination of the drying effect (Fig. 2) shows similar trends. We also found that the effect can be reversed by immersing the TBs in saline solution, thus the motion of the stapes recovers to approximately the same levels as before being dried. Such restoration of the mechanical properties of the middle-ear tissues by immersing the TBs in saline solution has been observed in other studies (Voss et al., 2000; Willi et al., 2002; Nakajima et al., 2005).

Artificial immobilization of the IMJ in this study was performed under the microscope by applying glue to the inner space of the IMJ capsule after removal of the synovial fluid. The effectiveness of the artificial immobilization procedures was confirmed by measurements of the relative motion between the malleus and incus before and after the artificial immobilization (Fig. 4). The relative motion was reduced by 10 to 15 dB after the artificial immobilization.

Our results indicate that a mobile IMJ attenuates the magnitude of middle-ear sound transmission, especially for frequencies above 2 kHz. The mean piston-like motion (*Voz*)

385 increases after immobilization by less than 7 dB for the frequencies from 1.8 to 8 kHz.
386 Specifically, the prominent difference occurs from 2 to 4 kHz, and at 5.5 kHz ($p < 0.01$ with
387 paired *t*-test). With the mobile IMJ, the ratios of the two rocking-like motions to the piston-
388 like motion were frequency-dependent ($p < 0.001$ with ANOVA test), that is to say, there
389 were relatively large rocking-like motions at higher frequencies. This is in agreement with
390 results from previous studies (Heiland et al., 1999; Hato et al., 2003; Sim et al., 2010). The
391 two ratios showed no significant difference between the mobile and immobilized IMJ
392 conditions, suggesting that there are no important changes in relative magnitude ratios of the
393 rocking-like motions to the piston-like motion caused by immobilization of the IMJ.
394 The larger difference of the piston-like stapes motion between the mobile and
395 immobilized IMJ conditions at higher frequencies is presumed to be due to relatively large
396 loss of motion from malleus to incus at higher frequencies for the normal IMJ as compared to
397 the immobilized IMJ. With the normal condition of the IMJ (i.e., before the IMJ
398 immobilization), the index for the ratio of the relative motion (R_{TOTAL}) increased with
399 frequency (Fig 3), indicating more relative motion at higher frequencies. Therefore, the
400 mobility of the IMJ will not affect the middle-ear sound transmission at low frequencies
401 considerably. At frequencies above 4 kHz, the R_{TOTAL} is maximized and reaches almost 0 dB
402 (i.e., ratio of 1), indicating that the magnitude of the relative motion is almost the same as the
403 average magnitude of the malleus motion and the incus motion. Therefore, in this frequency
404 range, the immobilization of the IMJ is expected to affect the middle-ear transmission
405 significantly.
406 The high-frequency dominant change in middle-ear sound transmission due to
407 mobility of the IMJ in human TBs has been described previously. Huber et al. (1997) reported
408 a transmission loss from the malleus to the incus of about 6 dB at frequencies above 2 kHz
409 under acoustic stimulation at moderate SPLs. Offergeld et al. (2007) observed an increase of
410 less than 10 dB in the amplitude of the stapes motion after immobilization of the IMJ for

411 frequencies from 1.2 - 5 kHz. Willi et al. (2003) described that a decrease of 5.5 dB per
412 octave above 1 kHz may be caused by the mobility of the IMJ, based on the transmission loss
413 observed in his two-dimensional measurements of motions of the malleus and the incus.
414 Mobility of the human IMJ has been found in many previous studies (Helmholtz,
415 1868; Mach and Kessel, 1874; Frank, 1923; Dahmann, 1930; Stuhlman, 1937; Kobrak, 1959;
416 Marquet, 1981; Schön and Müller, 1999; Huber et al., 1997; Decraemer and Khanna, 1999,
417 2001; Willi et al., 2002, 2003; Sim et al, 2004; Nakajima et al., 2005; Offergeld et al., 2007).
418 Decraemer et al. (2014) also observed large slippage in the IMJ in TBs, and addressed two
419 possible reasons for the slippage: 1) there are post-mortem changes in the cadaveric TBs that
420 were used to examine the mobility of the IMJ in most studies; 2) the cadaveric TBs are from
421 elderly people. They doubted that large slippage in the IMJ "really happens in the healthy
422 living ear (pp. 508)".
423 It is known that cadaveric TBs have fast and slow post-mortem changes. The *fast* post-
424 mortem changes, which are presumed to be caused mainly by a stoppage of blood flow and
425 changes of the inner ear pressure in cadaveric ears, occur immediately after death (Brenkman
426 and Grote, 1987). Békésy (1960), from his anatomical studies for human TBs, described that
427 no considerable change of the elasticity of the ligaments, the joint capsule or the tympanic
428 membrane occurs within several hours after death, indicating that the fast post-mortem
429 changes probably do not affect middle-ear mechanics significantly. Several other studies have
430 reported the fast post-mortem changes in animals as well, and found no considerable
431 difference from living animals up to 1 hour in guinea pigs (Gilad et al. 1967), 1-2 hours in
432 cats (Tonndorf and Khanna 1967, 1968), 17 hours in rabbits (Gill 1951), and 48 hours in
433 rabbits (Onchi 1961).
434 The *slow* post-mortem changes, which may be caused by dehydration and autolysis,
435 are important for the repeatability and stability of the measurements. According to previous
436 studies, the slow post-mortem changes do not necessarily occur in all human TBs, and the

437 effects are not accentuated for a specific frequency range. Goode et al. (1993) measured umbo
438 displacement 2 weeks and 4 weeks after death, and obtained almost the same frequency
439 responses. Rosowski et al. (1990) observed considerable post-mortem changes before 100
440 days only in two out of nine TBs investigated. Brenkman and Grote (1987) observed from
441 their measurement with two TBs that the umbo velocity was stable up to 45 hours after death
442 and then decreased with post-mortem time for the investigated frequencies of 0.6, 2 and 5
443 kHz. Zwislocki and Feldman (1963) observed that the changes start in the low-frequency
444 range. Effects of the slow post-mortem changes on the measurements in this study were
445 unavoidable. However, they were minimized by preserving the fresh TBs in thiomersal 0.1 %
446 solution at 4° C within 24 hours after death and by performing most measurements within a
447 week after death (with the exception of TB2, which was measured 13 days after the death).
448 No major differences in terms of stapes motion between live human subjects and fresh human
449 TBs were obtained in intraoperative measurements (Huber et al. 2001, Chien et al. 2009),
450 which strongly argues against large post-mortem effects. Therefore, our observation that the
451 immobilized IMJ generates larger piston-like motions than the mobile IMJ only at frequencies
452 above 2 kHz is not likely to be from the post-mortem changes of the TBs.
453 The fact that the temporal bones in this study are mostly from elderly subjects
454 (average of 68 years) could have influenced the results. Although we did not observe an age
455 dependency in our results, the number of samples is too small to draw a definitive conclusion.
456 Decraemer and Khanna (2004) noted that their experiments also may have been biased due to
457 use of temporal bones from elderly subjects. Willi (2003) describes a trend of a decrease of
458 sound transmission at higher frequencies (> 3 kHz) with age in fresh human temporal bones,
459 which would have to be confirmed in further measurements. Several morphological
460 parameters of the IMJ may change with age including hyalinization or calcification of the
461 joint capsule, thinning and calcification of the articular cartilage, thinning and calcification of
462 the disc, and arthritis resulting in narrowing or obliteration of the joint space (Gussen, 1971;

463 Etholm and Belal, 1974). In addition, the amount of elastic fibers in the joint capsule tends to
464 decrease with age (Harty, 1953), which may result in a reduction of the joint tension. Savić
465 and Djerić (1988) describe degenerative changes in 40 % of their samples from persons
466 between 40 and 60 years. While the reduction of the joint tension is expected to increase the
467 mobility of the IMJ, effects of other morphological changes such as calcification and
468 obliteration on the mobility of the IMJ have not been investigated, to our knowledge. With a
469 possibility that the age-related morphological changes of the IMJ increase its mobility, we
470 cannot rule out that the large mobility of the IMJ that we observed may have been due to the
471 TBs from elderly people used in this study.

472 Another possibility is that the mobility of the IMJ exists as part of a protection
473 mechanism, and the transmission loss at the high frequencies under moderate sound pressures
474 is an unavoidable side effect of this mechanism. That is, the mobility of the IMJ that exists to
475 protect the sensitive structures of the inner ear against high static pressure change also affects
476 normal sound transmission with acoustic sound simulation of moderate levels. The protection
477 mechanism has been proposed previously by several investigators (Dahmann, 1929, 1930;
478 Békésy, 1936; Stuhlman 1937; Kobrak, 1959; Hüttenbrink, 1988a, 1988b, 1997; Cancura,
479 1980; Offergeld et al., 2000).

480 Puria and Steele (2010) predicted that the mobility of the IMJ could provide flexible
481 adaptation to the complex motion of the malleus such as a twisting motion (i.e., rotational
482 motion about the superior-inferior axis) at high frequencies. However, our results that
483 artificial immobilization of the IMJ increased the middle-ear transfer function of the piston-
484 like motion without change in the pattern of the stapes motion do not provide evidence for
485 such a role of adaptation of the IMJ, at least up to 8 kHz, which is the frequency range
486 considered in this study.

5. Conclusion

The IMJ was shown to be mobile at frequencies above 2 kHz under physiologically relevant acoustic stimulation of 90-110 dB SPL. A prominent frequency-dependent difference of the piston-like motion of the stapes between the mobile and immobilized IMJ conditions was observed; whereas, the ratio of the rocking-like motions relative to the piston-like motion of the stapes showed no significant difference. The prominent frequency-dependent change of the piston-like motion above 2 kHz is presumed to be due to large mobility of the IMJ at high frequencies. It is still questionable whether the mobility of the IMJ exists as part of a protection mechanism, regardless of age, or occurs only in elderly people due to aging effects. Since the sample size of six in this study is not sufficient to reveal the effects of age on middle-ear sound transmission, further measurements are required to clarify these open questions.

Acknowledgement

This study was funded by SNF (Swiss National Foundation) Project No. 138726 and by DFG (German Research Council) Project No. EI 231/6-1. The authors thank Prof. B. Seifert, Division of Biostatistics, Institute of Social- and Preventive Medicine, University of Zurich for the statistical consulting.

505 ***References***

506 American Society for Testing and Materials (ASTM) F2504-05 (2005). Standard practice for
507 describing system output of implantable middle ear hearing devices. Philadelphia.

508 Békésy, von G., 1936. Zur Physik des Mittelohres und über das Hören bei fehlerhaftem
509 Trommelfell. Akust. Zeits. 1, 13–23.

510 Békésy, von G., 1941. Über die Messung Schwingungsamplitude der Gehörknöchelchen
511 mittels einer kapazitiven Sonde [About the vibration amplitude of the ossicles measured by
512 means of a capacitive probe] Akust Zeits. 6, 1–16.

513 Békésy, von G., 1960. Experiments in hearing. McGraw-Hill, New York.

514 Brenkman, C.J., Grote, J.J., 1987. Acoustic transfer characteristics in human middle ears
515 studied by a SQUID magnetometer method. J. Acoust. Soc. Am. 82, 1646-1654.

516 Cancura, W., 1980. On the statics of malleus and incus and on the function of the malleus-
517 incus joint. Acta Otolaryngol. 89 (3-4), 342-344.

518 Chien, W., Rosowski, J., J., Ravicz, M., E., Rauch, S., D., Smullen, J., Merchant, S., N., 2009.
519 Measurements of stapes velocity in live human ears. Hear. Res. 249, 54-61.

520 Dahmann, H., 1929. Zur Physiologie des Hörens; experimentelle Untersuchungen über die
521 Mechanik der Gehörknöchelchenkette, sowie über deren Verhalten auf Ton und Luftdruck.
522 Kongressbericht "zur Physiologie des Hörens". Z. Hals Nas. Ohrenheilkd. 24, 462-497.

523 Dahmann, H., 1930. Zur Physiologie des Hörens; Experimentelle Untersuchungen über die
524 Mechanik der Gehörknöchelchenkette sowie über deren Verhalten auf Ton und Luftdruck. Z.
525 Hals Nas. Ohrenheilkd. 27, 329-368.

526 Decraemer, W.F., Khanna, S.M., 1999. New insights in the functioning of the middle ear. In:
527 Rosowski, J.J., Merchant, S.N. (Eds.), The Function and Mechanics of Normal, Diseased and
528 Recon- structed Middle Ears. Kugler Publications, The Hague, 23-38.

529 Decraemer, W.F., Khanna, S.M., 2001. Complete 3-dimensional motion of the ossicular chain
530 in a human temporal bone. Abstract. Proceedings of the twenty-fourth Annual Midwinter
531 Research Meeting of the Association for Research in Otolaryngology 24, 221.

532 Decraemer, W.F., Khanna, S.M., 2004. Measurement, visualization and quantitative analysis
533 of complete three-dimensional kinematical data sets of human and cat middle ear. In: Gyo, K.,
534 Wada, H., Hato, N., Koike, T. (Eds.), Middle Ear Mechanics in Research and Otology. World
535 Scientific, Singapore. 3–10.

536 Decraemer W.F., Rochefoucauld O., Funnell W.R.J., Olson E.S., 2014. Three-dimensional
537 vibration of the malleus and incus in the living gerbil. Journal of the Association for Research
538 in Otolaryngology 15, 483-510.

539 Elpern, B.S., Greisen, O., Andersen, H.C., 1965. Experimental studies on sound transmission
540 in the human ear. VI. Clinical and Experimental Observations on Non-Otosclerotic Ossicle
541 Fixation. Acta Otolaryngol. 60 (1-6), 223-230.

542 Etholm, B., Belal, A., 1974. Senile changes in the middle ear joints. Ann. Otol. 83 (1), 49-54.

543 FICAT, 1998, Federative Committee on Anatomical Terminology (FICAT), International
544 Federation of Associations of Anatomists. Terminologia anatomica. Stuttgart: G. Thieme.

Frank, O., 1923. Die Leitung des Schalles im Ohr. Bayerische Akademie der Wissenschaften. 1923.

Gilad, P., Shtrikman, S., Hillmann, P., 1967. Application of the Mössbauer method to ear vibrations. J. Acoust. Soc. Am. 41, 1232-1236.

Gill, N.W., 1951. Some observations on the conduction mechanism of the ear. J. Laryngol. Otol. 65, 404-413.

Goode, R.L., Ball, G., Nishihara, S., 1993. Measurement of umbo vibration in human subjects - method and possible clinical applications. Am J Otol. 103 (5), 565-569.

Gyo, K., Aritomo, H., Goode, R.L., 1987. Measurement of the ossicular vibration ratio in human temporal bones by use of a video measuring system. Acta Otolaryngol. 103, 87-95.

Guinan, J.J., Peake, W.T., 1967. Middle-ear characteristics of anesthetized cats. J. Acoust. Soc. Am. 41, 1237-1261.

Gundersen, T., Hogmoen, K., 1976. Holographic vibration analysis of the ossicular chain. Acta Otolaryngol. 82, 16-25.

Gussen, R., 1971. The human incudomalleal joint. Chondroid articular cartilage and degenerative arthritis. Arthritis Rheum. 14, 465-74.

Harty, M., 1953. Elastic tissue in the middle-ear cavity. The Journal of laryngology and otology. 67, 723-729.

Harty, M., 1964. The joints of the middle ear. Z. Mikrosk. Anat. 71, 24-31.

Hato, N., Stenfelt, S., Goode, R.L., 2003. Three-dimensional stapes footplate motion in human temporal bones. Audiol Neurootol. 8, 140-152.

Heiland, K.E., Goode, R.L., Asai, M., Huber, A.M., 1999. A human temporal bone study of stapes footplate movement. AM J Otol. 20, 81-86.

Helmholtz, H. von, 1863. Die Lehre von den Tonempfindungen als physiologische Grundlage für die Theorie der Musik, [On the Sensations of Tone as a Physiological Basis for the Theory of Music], Sensations of Tone. J. Vieweg, Bayerische Staatsbibliothek.

Helmholtz, H. von, 1868. Die Mechanik der Gehörknöchelchenkette und des Trommelfells. Pflüg. Arch. 1, 1-60.

Huber, A., Assai, M., Ball, G., Goode, R. L., 1997. Analysis of ossicular vibration in three dimensions. In: Middle ear mechanics in research and otosurgery. Dresden. 82-87.

Huber, A., Linder, T., Ferrazzini, M., Schmid, S., Dillier, N., Stoeckli, S., Fisch, U., 2001. Intraoperative assessment of stapes movement. Ann Otol Rhinol Laryngol. 110(1), 31-35.

Hüttenbrink, K.B., 1988a. Die Mechanik der Gehörknöchelchen bei statischen Drucken. I.: Normales Mittelohr. Z. Laryngol. Rhinol. Otol. 67 (3), 45-52.

Hüttenbrink, K.B., 1988b. Die Mechanik der Gehörknöchelchenkette bei statischen Drucken. II: Behinderte Gelenkfunktion und operative Kettenkonstruktion. Laryngol. Rhinol. Otol. 67, 100-105.

Hüttenbrink, K.B., 1997. The middle ear as a pressure receptor. Middle ear mechanics in research and otosurgery. In: Hüttenbrink, K.B. (ed) Proc. Internat. Workshop, Dresden, 1996

584 Sep 19–22. Dept. Oto-rhinolaryngol., Univ. Hosp. Carl Gustav Carus, Dresden Univ.
585 Technology. 15–20.

586 Hüttenbrink, K.B., Pfautsch, M., 1987. Die Gelenke der Gehörknöchelchen im
587 rasterelektronen-mikroskopischen Bild. Laryngol. Rhinol. Otol. 66 (4), 176-179.

588 Kirikae, I., 1960. The Structure and Function of the Middle Ear. The University of Tokyo
589 Press.

590 Kobrak, H.G., 1959. The Middle Ear. University of Chicago Press.

591 Lauxmann, M., Eiber, A., Heckeler, C., Ihrle, S., Chatzimichalis, M., Huber, A.M., Sim, J.H.,
592 2012. In-plane motion of the stapes in human ears. J. Acoust. Soc. Am. 132 (5), 3280-3291.

593 Mach, E., Kessel, J., 1874. Beiträge zur Topographie und Mechanik des Mittelohres. Sitz. ber.
594 Kais. Akad. Wiss. Math. Nat. wiss. Kl. 3, 221-245.

595 Marquet, J., 1981. The incudo-malleal joint. J. Laryngol. Otol. 95, 543-565.

596 Nakajima, H.H., Ravicz, M.E., Merchant, S.N., Peake, W.T., Rosowski, J.J., 2005.
597 Experimental ossicular fixations and the middle ear's response to sound: evidence for a
598 flexible ossicular chain. Hear. Res. 204 (1-2), 60-77.

599 Offergeld, C.F.E., Hüttenbrink, K.B., Zahnert, T., Hoffmann, G., 2000. Experimental
600 investigations of ossicular joint ankylosis. In: Rosowski, J.J. and Merchant, S.N. (eds.), The
601 function and mechanics of normal, diseased and reconstructed middle ears. Kurger
602 Publication, The Hague, The Netherlands, 177-186.

603 Offergeld, C.F.E., Lasurashvili, N., Bornitz, M., Beleites, T., Zahnert, T., 2007. Experimental
604 investigations on the functional effect of ossicular joint fixation. In: Huber, A. and Eiber, A.
605 (eds.), The 4th Symposium on Middle Ear Mechanics in Research and Ootology. World
606 Scientific Publishing, Singapore. 102-108.

607 Onchi, Y., 1961. Mechanism of the middle ear. J. Acoust. Soc. Am. 33, 794-805.

608 Politzer A, 1873. Zur physiologischen Akustik und deren Anwendung auf die Pathologie des
609 Gehörorgans. Arch Ohrenheilkd. 6, 35-44.

610 Politzer, A., 1884. Traité des Maladies de l'Oreille. Paris, ed. Octave Doin.

611 Puria, S, Steele, C.R., 2010. Tympanic-membrane and malleus-incus-complex co-adaptions
612 for high–frequency hearing in mammals. Hear. Res. 263, 183-190.

613 Rosowski, J.J., Davis, P.J., Merchant, S.N., Donahue, K.M., Coltrera, M.D., 1990. Cadaver
614 middle ears as models for living ears: comparisons of middle-ear input immittance. Ann. Otol.
615 Rhinol. Laryngol. 99, 403–412.

616 Savić, D., Djerić, D., 1988. Histopathological characteristics of degenerative modifications of
617 the incudomalleolar joint. Ann Otolaryngol Chir Cervicofac. 105, 203-6.

618 Schön, F., Müller, J., 1999. Measurements of ossicular vibrations in the middle ear. Audiol.
619 Neurootol. 4 (3-4), 142-149.

620 Schuknecht, H.F., 1974. Pathology of the ear. Cambridge, Mass.: Harvard University Press.

621 Sim, J.H., Chatzimichalis, M., Lauxmann, M., Röösli, C., Eiber, A., Huber, A.M., 2010.
622 Complex stapes motions in human ears. J Assoc Res Otolaryngol. 11 (3), 329-341.

623 Sim, J.H., Chatzimichalis, M., Röösli, C., Laske, R.D., Huber, A.M., 2012. Objective
624 assessment of stapedotomy surgery from round window motion measurement. Ear & Hearing.
625 33 (5), 24-31.

626 Sim, J.H., Puria, S., 2008. Soft tissue morphometry of the malleus-incus complex from micro-
627 CT imaging. J Assoc Res Otolaryngol. 9, 5-21.

628 Sim, J.H., Puria, S., Steele, C.R., 2004. Three-dimensional measurement and analysis of the
629 isolated malleus-incus complex. In: Gyo K and Wada H (eds.), The 3rd International
630 Symposium on Middle Ear Mechanics in Research and Otology. World Scientific Publishing,
631 Singapore. 61-67.

632 Sim J.H., Röösli C., Chatzimichalis M., Eiber A. and Huber A.M., Characterization of stapes
633 anatomy: investigation of human and guinea pig, J. Assoc. Res. Otolaryngol. 14 (2), 2013,
634 159-73.

635 Stuhlman, O., 1937. The nonlinear transmission characteristics of the auditory ossicles. J.
636 Acoust. Soc. Am. 9, 119-128.

637 Tonndorf, J., Khanna, S.M., 1967. Some properties of sound transmission in the middle and
638 outer ears of cats. J. Acoust. Soc. Am. 41, 513–521.

639 Tonndorf, J., Khanna, S.M., 1968. Submicroscopic displacement amplitudes of the tympanic
640 membrane (cat) measured by a Laser interferometer. J. Acoust. Soc. Amer. 44, 1546-1554.

641 Voss, S.E., Rosowski J.J., Merchant, S.N., Peake, W.T., 2000. Acoustic responses of the
642 human middle ear. Hear. Res. 150, 43-69.

643 Willi, U.B., 2003. Middle-ear mechanics: the dynamic behavior of the incudo-malleolar joint
644 and its role during the transmission of sound. Doctoral Thesis in Mathematics and Natural
645 Science. University of Zurich, Zurich.

646 Willi, U.B., Ferrazzini, M.A., Huber, A.M., 2002. The incudo- malleolar joint and sound
647 transmission losses. Hear. Res. 174 (1-2), 32–44.

648 Zwislocki, J., Feldman. A.S., 1963. Post-mortem acoustic impedance of human ears. J.
649 Acoust. Soc. Am. 35, 104- 107.

650 **Figure Captions**

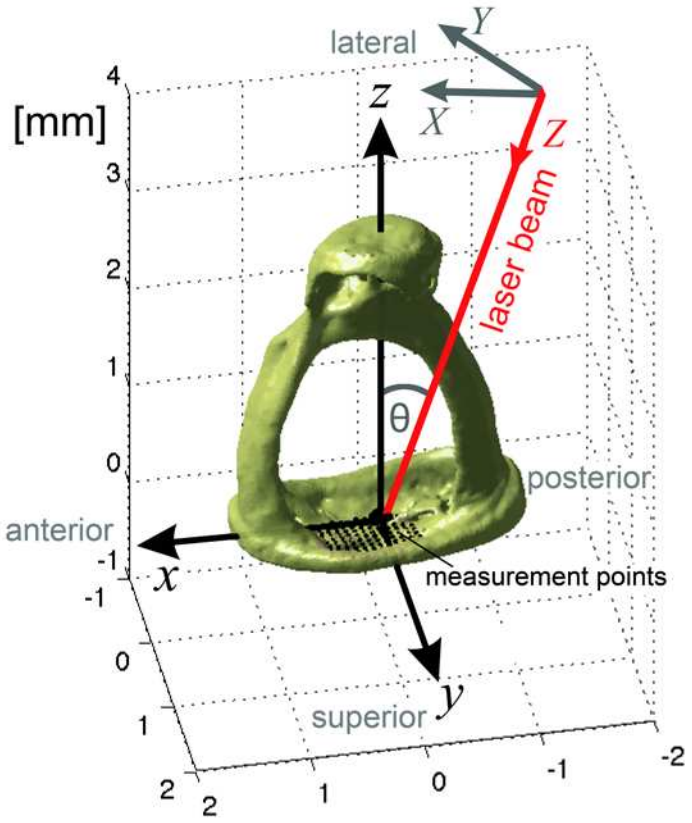

651
652 **Fig. 1** SLDV measurement frame (*XYZ* coordinate system) and footplate-fixed anatomical
653 frame (*xyz* coordinate system) for the right ear (right-handed frame system). In the SLDV
654 measurement frame, the *XYZ* coordinate system was set such that the laser beam was along
655 the *Z* direction and the *XY* plane was normal to the laser beam. In the footplate-fixed
656 anatomical frame, the *xy*-plane was fitted to the median surface of the stapes footplate, and the
657 origin at the centroid of the median surface. The anterior direction was set as the positive *x*-
658 direction, the superior direction as the positive *y*-direction, and lateral direction as the positive
659 *z*-direction. The angle θ between the laser beam direction (i.e., *Z* axis of SLDV frame) and the
660 *z* axis of the anatomical frame was 34 ± 11 °.
661

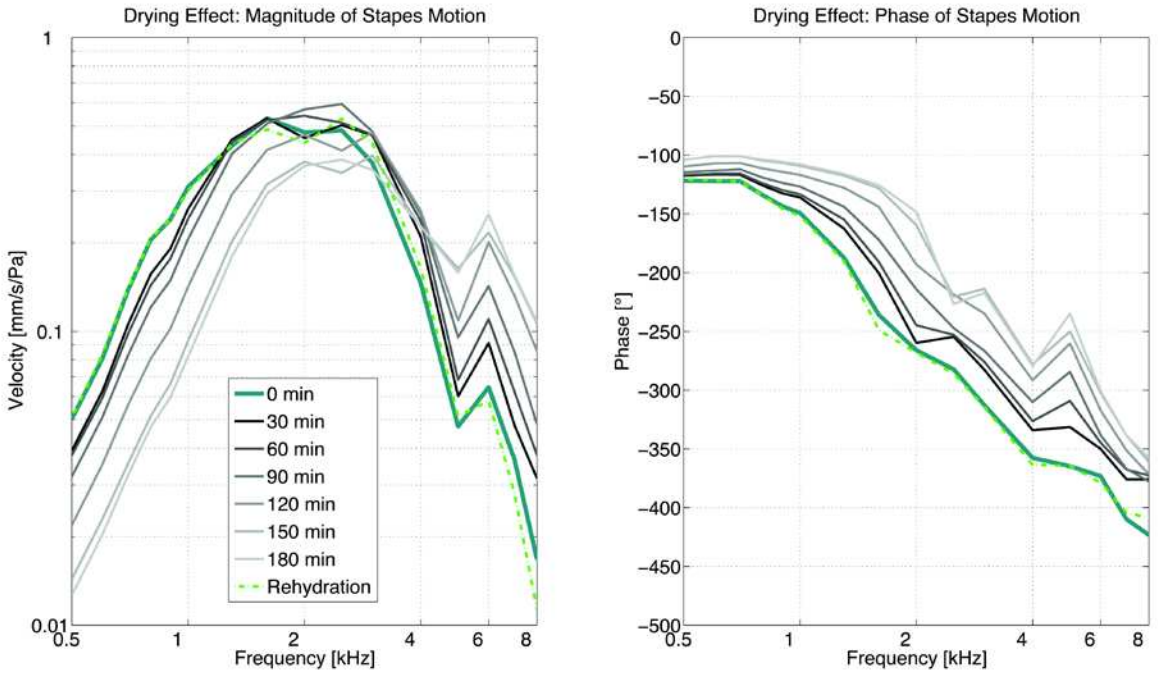

Fig. 2 Changes in the magnitudes (left) and phases (right) of motions of the stapes footplate (center) with drying. After the sample was dried for 180 minutes, it was rehydrated by immersion in saline solution.

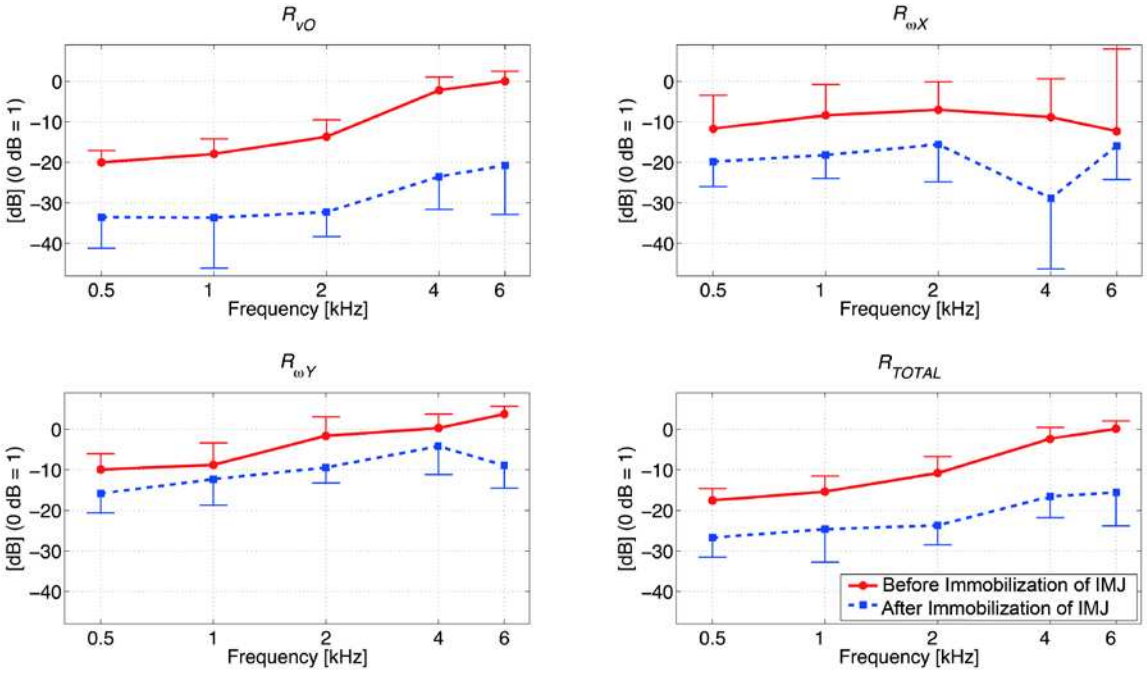

Fig. 3 Relative motion between the malleus and incus represented by the ratios of the relative motion components to the corresponding motion components of the malleus and incus, before IMJ was immobilized (solid) and after the IMJ was immobilized (dashed). The relative motion ratios for V_O (R_{vO}, left upper), ω_X ($R_{\omega X}$, right upper),, ω_Y ($R_{\omega Y}$, left below), and average with the ratio components weighted by portions of the corresponding motion components (R_{TOTAL}, right below). The ratio of 1 (= 0 dB) indicates that the magnitude of the relative motion component is the same as the average magnitude of the corresponding malleus motion component and the corresponding incus motuion component.

677

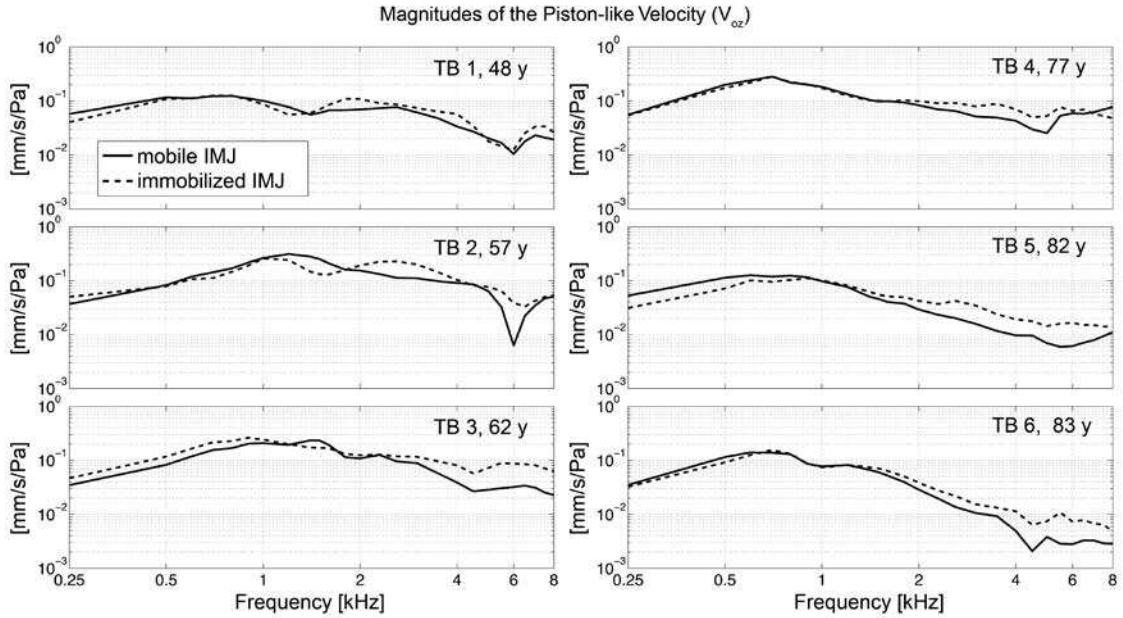

678

679 **Fig. 4** Magnitudes of the translational motions of the footplate center along the *z*-axis (i.e.,
680 piston-like motions, V_{oz}) normalized by the ear canal pressure, before (solid) and after
681 (dashed) the IMJ is immobilized.

682

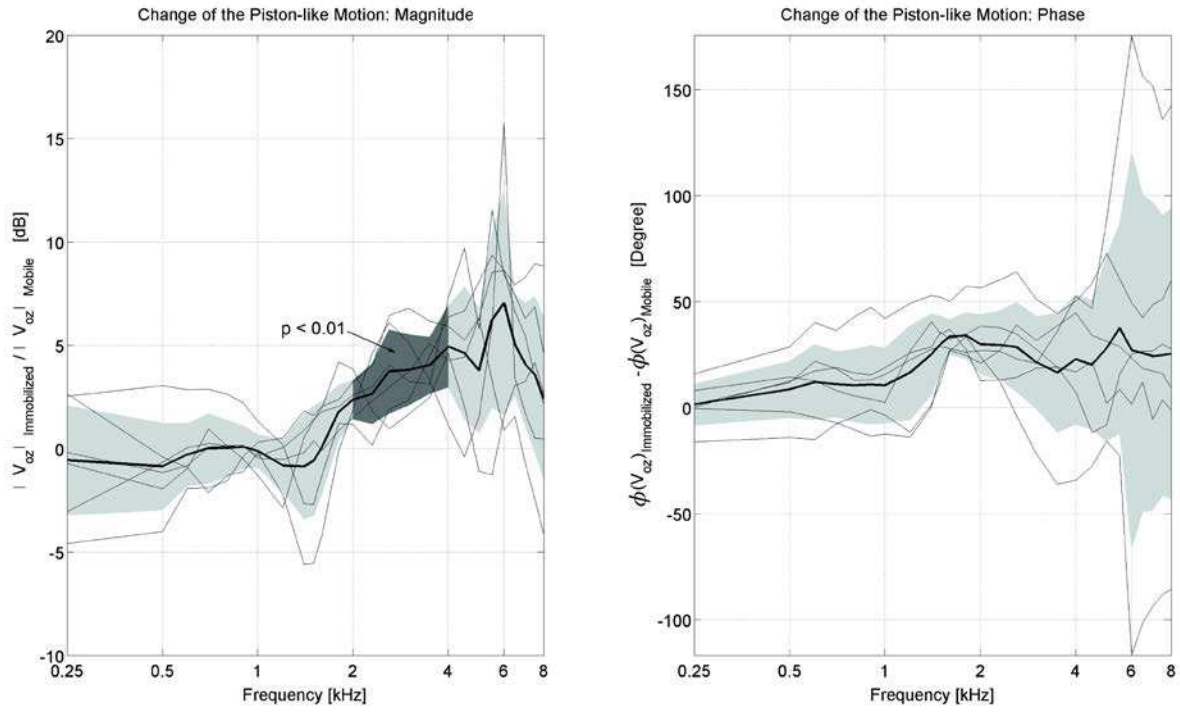

683

684 **Fig. 5** Change of the translational motion with immobilized IMJ relative to the translational
685 motion with mobile IMJ. Relative magnitude ratios (left) and relative phase difference (right)
686 with the mean values (thick lines) and standard deviations (shaded). Prominent differences in
687 magnitude between the mobile and immobilized conditions of the IMJ are shown as shaded
688 with dark gray (2- 4 kHz and 5.5 kHz, $p < 0.01$ with paired *t*-test).

689

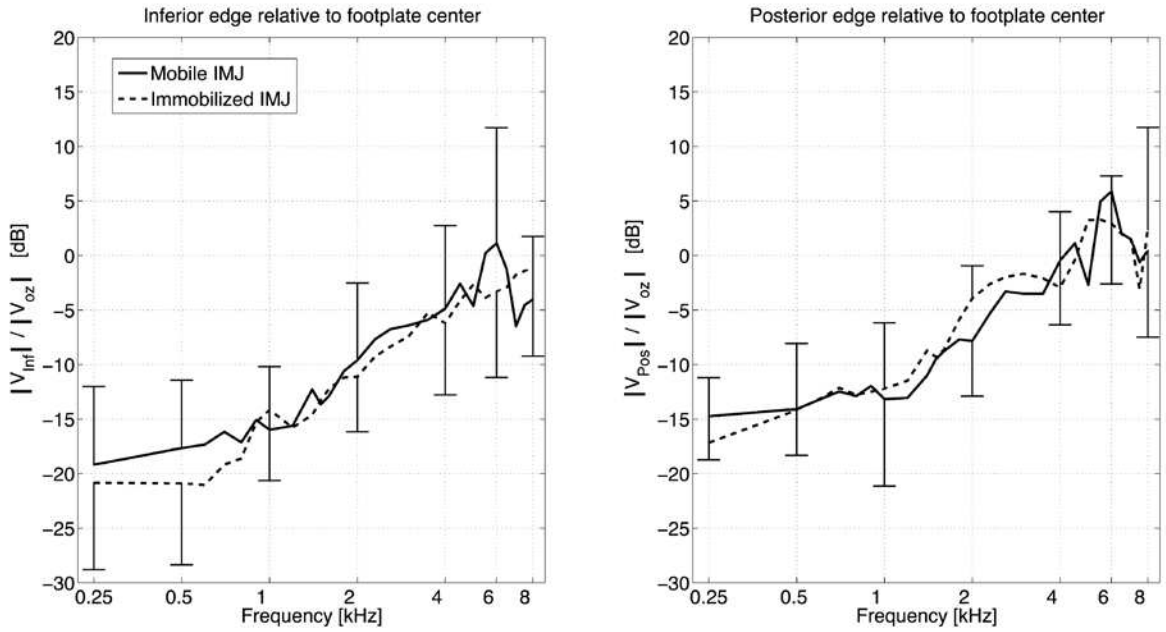

690

691 **Fig. 6** Relative magnitudes of the edge velocities generated by the rocking-like motions (i.e,
692 two rotational motions along the long and short axes of the footplate) with respect to the
693 piston-like motion (i.e., the footplate-center velocity in the *z*-direction), before (solid) and
694 after (dashed) the IMJ immobilization. The inferior-edge velocity due to the rocking-like
695 motion of the footplate along the long axis (left), and the posterior-edge velocity due to the
696 rocking-like motion of the footplate along the short axis (right).